Electronic Supplementary information

Template-assisted strategy to synthesis dilute CoNi alloy incorporated into ultramicroporous carbon for high performance supercapacitors application

Yan Jiang[1], Yue Wang[1], Dehong Zeng[1], Yao Wang[1], Yangde Ma[1], Hai Wang[2], Xin Zhang[1]*, Xiaoping Dai[1]

[1]State Key Laboratory of Heavy Oil Processing, China University of Petroleum, Changping, Beijing 102249, China

[2]National Institute of Metrology, Beijing 100013, P. R. China

Synthesis of SBA-15: SBA-15 was synthesized using tri-block copolymer (P123) as a soft template. Typically, 2.0 g P123 was dissolved in 60 mL of 2M HCl and 15 ml of distilled water at 40 ℃, and then the mixture was stirred for 1 h. After that, 4.17 mL of tetraethyl orthosilicate (TEOS) was added. The gel composition P123: HCl: H_2O: TEOS was 0.017: 5.88: 197: 1 in molar ratio. The resulting mixture was further stirred at 40 ℃ for 5 h, and then transferred into a teflon-lined stainless steel autoclave and aged at 100 ℃ for 24 h. After cooling down to room temperature, the products were filtered, washed with distilled water repeatedly, and dried overnight at 60 ℃ in air. The as-synthesized sample was then pyrolyzed in an air flow at 550 ℃ (heating rate 1 ℃ min^{-1}) and kept under these conditions for 6 h to remove the copolymer template.

Materials Characterization. The infrared spectra of samples were recorded in KBr disks using a Nicolet Nexus 870 FT-IR spectrometer. Powder X-ray diffraction (XRD) patterns of the samples were recorded on a Bruker D8-advance X-ray powder diffractometer operated at voltage of 40 kV and current of 40 mA with CuK radiation (λ = 1.5406 Å). The Raman spectra of samples were recorded with a HORIBA Jobin Yvon HR800 with a microscope attachment. The laser wavelength of 532 nm was focused using a diffraction limited spot, and the scan time was 2 s for each sample. The morphologies of samples were characterized by scanning electron microscope (SEM, FEI-Quanta 200F) at 15 kV and a transmission electron microscope (TEM, JEM-2100F) at 200 kV with an energy-dispersive X-ray spectrometry (EDS) equipment. The TEM images, selected area electron diffractions, high angle annular dark field scanning transmission electron microscopy (HAADF-STEM), line scanning

and mapping of C, Co and Ni elements were analyzed using a Tecnai G2 F20 S-Twin high-resolution transmission electron microscope (HRTEM) operating at 200 kV. N_2 adsorption/desorption isotherms were obtained by a Kubo X10000 static volumetric gas adsorption analyzed at -196 ℃. Before measurements, the samples were de-gassed at 300 ℃ for 3 h in vacuum. The specific surface area was calculated from the adsorption branches in the relative pressure range of 0.05-0.20 by the Brunauer-Emmett-Teller (BET) method. The mesopore size distribution was calculated from desorption branches by the Barret-Joyner-Halenda (BJH) method, and the single point adsorption total pore volume was taken at the relative pressure of 0.96. The micropore volume was calculated by *t-plot* method and the micropore size distribution was estimated by the Horvath-Kawazoe (H-K) method. The total reflection X-ray fluorescence (TXRF) was recorded on a Rigaku at 50 kV and 0.60 mA to measure the actual loading of cobalt and nickel. Hydrogen temperature-programmed reduction (H_2-TPR) was performed from room temperature to 800 ℃ using a homemade apparatus equipped with a thermal conductivity detector.
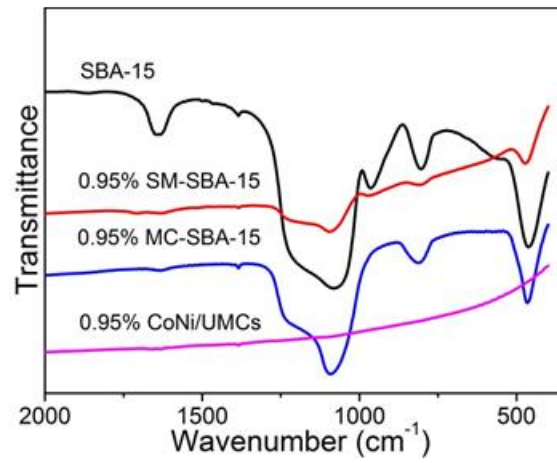
Figure S1. FT-IR spectra of SBA-15, 0.95% SM-SBA-15, 0.95% MC-SBA-15 and

0.95% CoNi/UMCs.
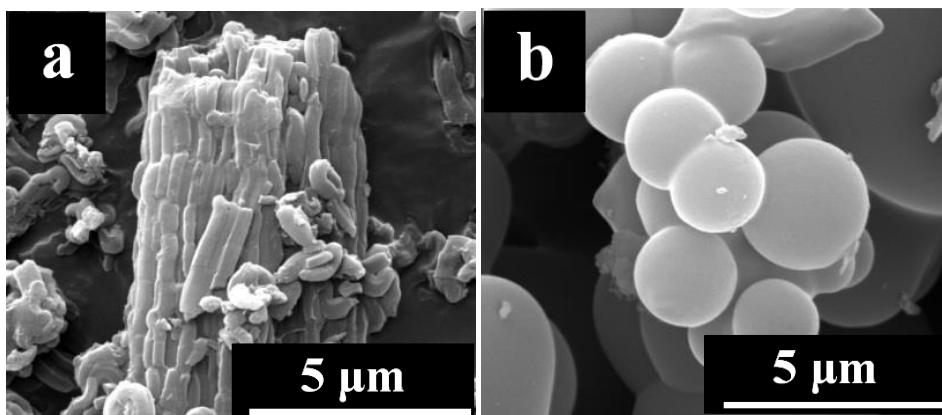
Figure S2 (a) SEM image of 0.95%CoNi/CMK-3, (b) SEM image of 0.95%CoNi/UMCs-2.

Table S1 The actual mass ratio of Co/C and Ni/C measured by TXRF characterization.

Samples	Co(Ac)$_2$ 4H$_2$O[a]	Co/C[b]	Ni(Ac)$_2$ 4H$_2$O[c]	Ni/C[d]
	(mg)		(mg)	
UMCs	0	0	0	0
0.11% CoNi/UMCs	16	0.11%	16	0.09%
0.50% CoNi/UMCs	20	0.50%	20	0.55%
0.95% CoNi/UMCs	24	0.95%	24	0.98%
1.04% CoNi/UMCs	32	1.04%	32	1.10%

[a] The mass of Co(Ac)$_2$ 4H$_2$O in the process of synthesis CoNi/UMCs composites;

[b] The actual mass ratio of Co/C measured by TXRF characterization;

[c] The mass of Ni(Ac)$_2$ 4H$_2$O in the process of synthesis CoNi/UMCs composites;

[d] The actual mass ratio of Ni/C measured by TXRF characterization.
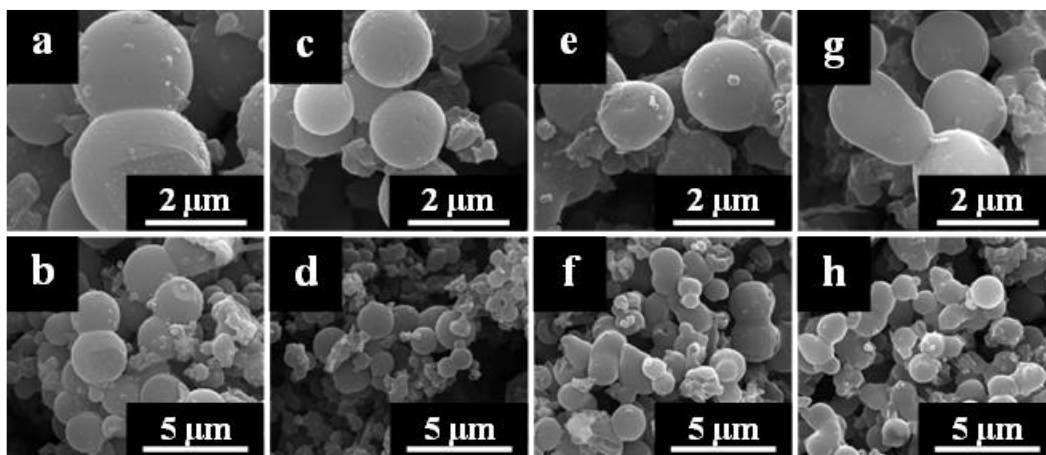
Figure S3. SEM images of (a, b) UMCs, (c, d) 0.11% CoNi/UMCs, (e, f) 0.50% CoNi/UMCs, (g, h) 1.04% CoNi/UMCs.

(b)

Element	Wt%	Co/Ni
CoK	00.10	1.11
NiK	00.09	

(d)

Element	Wt%	Co/Ni
CoK	00.48	0.96
NiK	00.50	

(f)

Element	Wt%	Co/Ni
·CoK	00.94	0.97
·NiK	00.97	

(h)

Element	Wt%	Co/Ni
·CoK	01.11	0.90
·NiK	01.23	
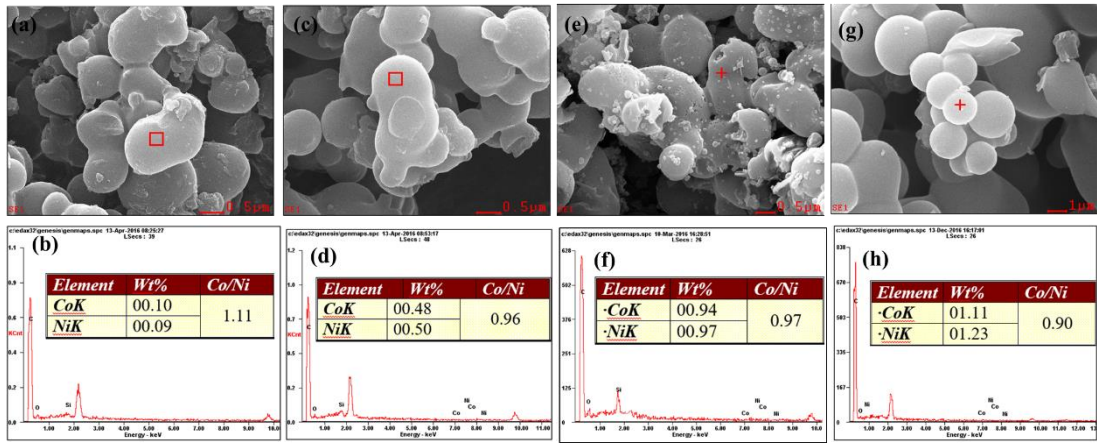
Figure S4 SEM images and EDX mapping of (a)(b) 0.11%, (c)(d) 0.50%, (e)(f) 0.95%, (g)(h) 1.04%CoNi/UMCs.
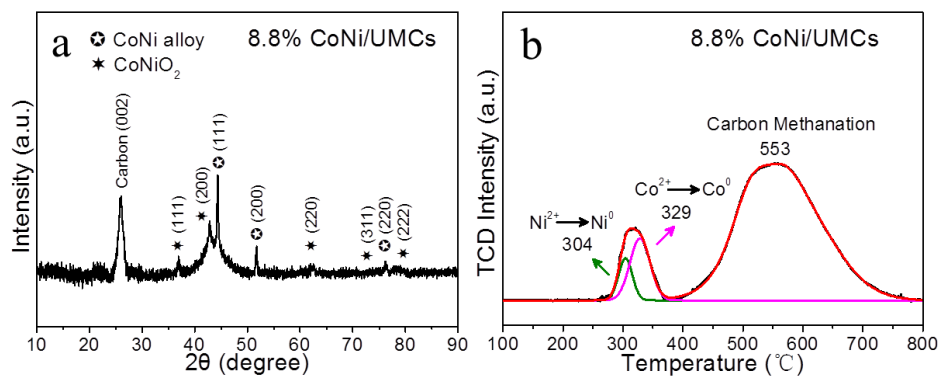
Figure S5. (a) XRD patterns, (b) H$_2$-TPR profiles of 8.8% CoNi/UMCs.

Table S2 The peak temperatures and H_2 consumption of CoNi/UMCs composites.

Samples	Peak temperatures (°C)	H_2 consumption (mmol)
UMCs	648	0.026
0.11% CoNi/UMCs	547	0.016
0.50% CoNi/UMCs	576	0.028
0.95% CoNi/UMCs	590	0.032
1.04% CoNi/UMCs	627	0.029

Table S3 A comparison of as-prepared 0.95% CoNi/UMCs with other ultramicro-, micro- and mesoporous carbons as electrode materials for EDLCs in aqueous electrolyte.

Materials		Specific capacitance (F g^{-1})				Ref.
		0.25 A g^{-1}	0.50 A g^{-1}	1.00 A g^{-1}	10 A g^{-1}	
Ultramicroporous carbon	0.95% CoNi/UMCs	268	251	241	-	this work
	UCNs	-	222	206	156	1
	PVFC	-	218	194	133	2
	UCM-1	-	~ 300	-	-	3
	UMCN-60	-	411	-	238	4
Microporous carbons	C800	~ 200	-	-	-	5
	NPC	258	-	-	-	6
Mesoporous carbons	CMK-3	-	-	210	126	7
	FDU-15	-	130	119	100	8
	MC-1	-	208	-	~ 170	9
	HPC-bdc	170	-	-	-	10
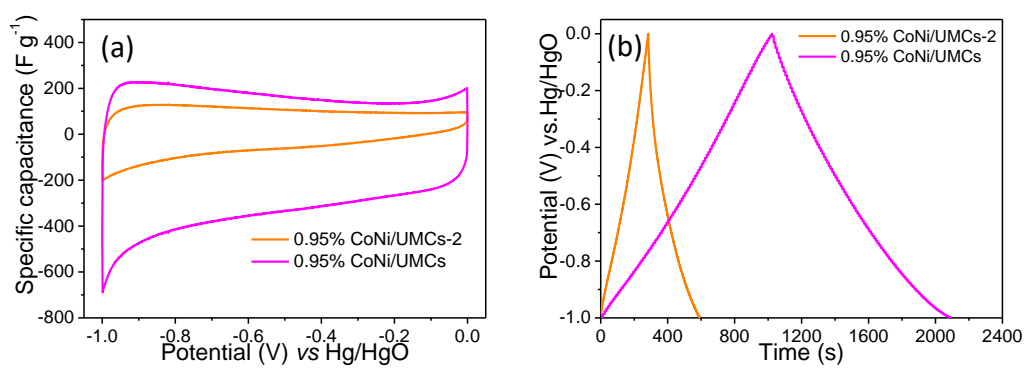
Figure S6. Capacitive performance: (a) CV curves at 1 mV s^{-1} and (b) GCD curves at 0.25 A g^{-1} of 0.95% CoNi/UMCs-2 and 0.95% CoNi/UMCs.
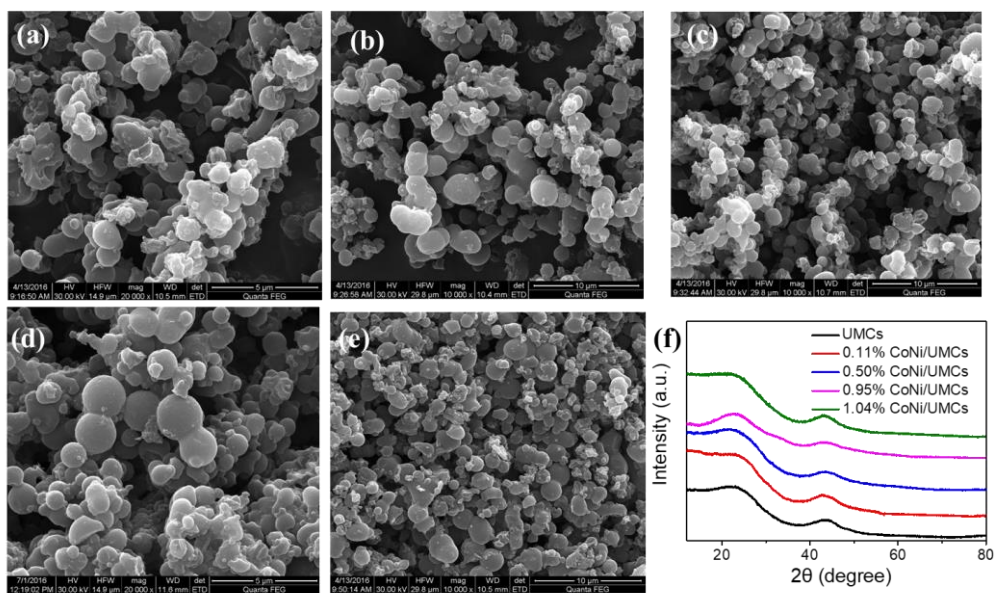
Figure S7 SEM images of (a) UMCs, (b) 0.11%, (c) 0.50%, (d) 0.95%,

(e)1.04%CoNi/UMCs; and (f) XRD patterns of the composites.
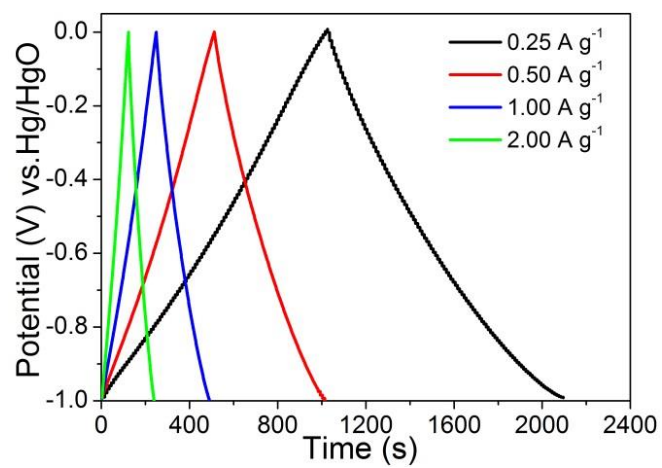
Figure S8. GCD curves at different current densities of 0.95% CoNi/UMCs.
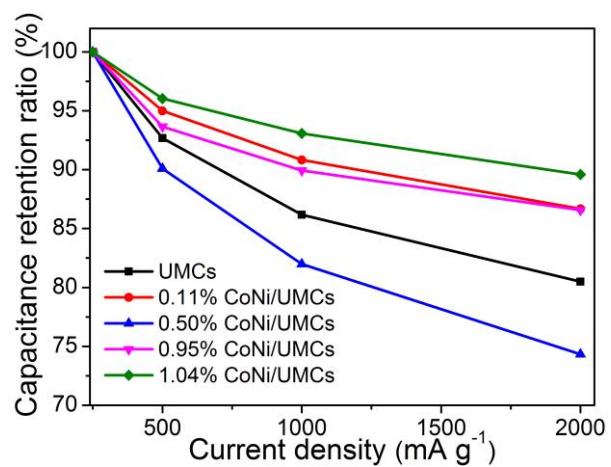
Figure S9. Capacitance retention ratios as a function of current densities of CoNi/UMCs composites in 6 M KOH.

REFERENCES

(1) Zhao, Y.; Liu, M.; Gan, L.; Ma, X.; Zhu, D.; Xu, Z.; Chen, L., Ultramicroporous Carbon Nanoparticles for the High-Performance Electrical Double-Layer Capacitor Electrode. *Energy & Fuels* **2014,** *28* (2), 1561-1568.

(2) Xu, B.; Hou, S.; Duan, H.; Cao, G.; Chu, M.; Yang, Y., Ultramicroporous carbon as electrode material for supercapacitors. *Journal of Power Sources* **2013,** *228* (11), 193-197.

(3) Yun, Y. S.; Lee, S.; Kim, N. R.; Kang, M.; Leal, C.; Park, K. Y.; Kang, K.; Jin, H. J., High and rapid alkali cation storage in ultramicroporous carbonaceous materials. *Journal of Power Sources* **2016,** *313*, 142-151.

(4) Liu, M.; Qian, J.; Zhao, Y.; Zhu, D.; Gan, L.; Chen, L., Core-shell ultramicroporous@microporous carbon nanospheres as advanced supercapacitor electrodes. *Journal of Materials Chemistry A* **2015,** *3* (21), 11517-11526.

(5) Jiang, H. L.; Liu, B.; Lan, Y. Q.; Kuratani, K.; Akita, T.; Shioyama, H.; Zong, F.; Xu, Q., From metal-organic framework to nanoporous carbon: toward a very high surface area and hydrogen uptake. *Journal of the American Chemical Society* **2011,** *133* (31), 11854-7.

(6) Liu, B.; Shioyama, H.; Akita, T.; Xu, Q., Metal-organic framework as a template for porous carbon synthesis. *Journal of the American Chemical Society* **2008,** *130* (16), 5390-1.

(7) Luo, H.; Zheng, L.; Lei, L.; Zhang, D.; Wu, J.; Yang, J., Supercapacitive behavior of mesoporous carbon CMK-3 in calcium nitrate aqueous electrolyte. *Korean Journal of Chemical Engineering* **2014,** *31* (4), 712-718.

(8) Lv, Y.; Zhang, F.; Dou, Y.; Zhai, Y.; Wang, J.; Liu, H.; Xia, Y.; Tu, B.; Zhao, D., A comprehensive study on KOH activation of ordered mesoporous carbons and their supercapacitor application. *Journal of Materials Chemistry* **2011,** *22* (1), 93-99.

(9) Li, Q.; Jiang, R.; Dou, Y.; Wu, Z.; Huang, T.; Feng, D.; Yang, J.; Yu, A.; Zhao, D., Synthesis of mesoporous carbon spheres with a hierarchical pore structure for the electrochemical double-layer capacitor. *Carbon* **2011,** *49* (4), 1248-1257.

(10) Yang, Y.; Hao, S.; Zhao, H.; Wang, Y.; Zhang, X., Hierarchically porous carbons derived from nonporous metal-organic frameworks: Synthesis and influence of struts. *Electrochimica Acta* **2015,** *180*, 651-657.